Electrostatic instability of some jellium model lattices of high symmetry to their plane cleavage

2007 J. Phys.: Condens. Matter 19 086216

(http://iopscience.iop.org/0953-8984/19/8/086216)

IOP PUBLISHING JOURNAL OF PHYSICS: CONDENSED MATTER

J. Phys.: Condens. Matter **19** (2007) 086216 (17pp) doi:10.1088/0953-8984/19/8/086216

Electrostatic instability of some jellium model lattices of high symmetry to their plane cleavage

Eugene V Kholopov[1] **and Vita V Kalashnikova**[1,2]

[1] A V Nikolaev Institute of Inorganic Chemistry, Siberian Branch, Russian Academy of Sciences, 630090 Novosibirsk, Russia
[2] Novosibirsk State University, 630090 Novosibirsk, Russia

E-mail: kholopov@che.nsk.su

Received 17 July 2006, in final form 19 December 2006
Published 9 February 2007
Online at stacks.iop.org/JPhysCM/19/086216

Abstract

Jellium model structures composed of regular lattices of equal point charges immersed in a neutralizing uniform background are considered. The symmetric description eliminating the effect of potentials without transverse structural modulation is extended to the events specified by alternating distances between point-charge planes. Based on modulated potentials typical of plane-wise lattice summation, the energy of interaction between two semi-infinite hemi-crystals divided by a plane is obtained for cubic and hexagonal crystals, where all the characteristic orientations of the cleavage plane are taken into account. We found that simple cubic and hexagonal lattices, as well as cubic and hexagonal diamond structures, turn out to be unstable for certain cleavage planes. The most favourable cleavage planes for the bcc, fcc and hcp structures are also emphasized.

1. Introduction

The approach based on jellium models was first put forward in connection with the problem of lattice summation of Coulomb series [1–3]. However, it also appears to be fruitful upon describing different electron properties of metals [4–7]. Its simplicity accounts for many efforts to improve such a treatment so as to make it more realistic for certain applications [8, 9]. The interest in jellium models remains upon describing different bulk properties [10–14], including the interaction with impurities [15, 16] that is, for instance, inherent in the modern hydrogen storage problem [17–19]. Such models are used upon examining peculiar features of finite slabs [20], as well as for describing quantum size effects [21–26]. Different surface properties [10, 13, 27–38] and the interaction between surfaces [39, 40] are successfully investigated within the framework of jellium models as well.

The problems of stability within the jellium model treatment are of special interest. The classical topic is associated with the uniform electron gas immersed in a neutralizing

uniform background, where the instability with respect to the Wigner crystallization is predicted [41–44]. It is significant in this respect that the negative bulk Coulomb energy actually warrants the stability of a system. In particular, different aspects of lattice stability as a bulk property have been studied, evaluating the predominant Coulomb contribution in a jellium model [45, 46].

However, it turns out that there is one more source of instability driven by the application of a jellium model to crystals. This fact was noticed by Lang and Kohn [5] in the particular case of a simple cubic lattice with the $(1, 0, 0)$ plane surface. In this case the electrostatic contribution to the surface energy appears to be negative. Obtained within a jellium model, this result implies the repulsion between two semi-infinite parts of a crystal and so one more sort of bulk instability. On the other hand, it is evident that this effect is artificial. It seems important to understand whether there are other structures with such a property.

In the present paper we consider four cubic and three hexagonal point structures immersed in a neutralizing uniform background. The most symmetric orientations of the cleavage plane are examined. The plane-wise summation is adopted to obtain the analytic results for the interaction energy mentioned above. We show that the unstable simple cubic lattice is not unique.

2. Potential contributions of a single neutral symmetric layer

Interested in a certain energy effect of Coulomb nature in jellium models, we begin with the characteristic potentials generated by plane structural fragments treated as unit ones. In the simplest case such a unit contains one plane lattice composed of equal point charges q, with the elementary vectors $\mathbf{a}_1 = a_1\mathbf{e}_1$ and $\mathbf{a}_2 = a_2\mathbf{e}_2$ of lattice translations. Here $\mathbf{e}_1$ and $\mathbf{e}_2$ are the respective unit vectors with the product $(\mathbf{e}_1\mathbf{e}_2) = \cos\theta$. The crystal is then assumed to be constituted of such parallel planes separated by a distance c in the normal direction, providing that this set of planes is immersed in a neutralizing uniformly charged background. Thus, the area of a unit mesh per charge in a plane is equal to $s = a_1a_2\sin\theta$, the unit cell volume $v = sc$ and the charge density of a background $\rho = -q/v$.

Following Sholl [47], it is reasonable to single out an electrically neutral layer fragment associated with a sole plane in a symmetric manner, as shown at the top in figure 1(a). The translational symmetry in a plane, along with the uniform background effect, implies that the potential of the layer in question can be decomposed into two parts, uniform and modulated in the plane directions, respectively.

The uniform part $\phi_0(z)$ can be easily obtained as a solution of the corresponding boundary-value problem, that is defined by the following relations:

$$\frac{\mathrm{d}^2\phi_0(z)}{\mathrm{d}z^2} = -4\pi\rho, \qquad \frac{\mathrm{d}\phi_0(z)}{\mathrm{d}z}\Big|_{z=0\pm} = \mp\frac{2\pi q}{s}, \qquad \phi_0\left(\pm\frac{c}{2}\right) = 0, \tag{1}$$

because a variable z normal to the plane of the layer is essential alone. The solution $\phi_0(z)$ can be readily obtained from this. Making use of the mean potential value $\bar{\phi}_0 = \pi qc/(6s)$ appropriate to the case, the modified potential $\phi_0^{\mathrm{mod}}(z) = \phi_0(z) - \bar{\phi}_0$, that is reconciled with the Ewald approach [47], takes the form

$$\phi_0^{\mathrm{mod}}(z) = \begin{cases} \dfrac{2\pi qc}{s}\left[\left(\dfrac{1}{2} - \dfrac{|z|}{c}\right)^2 - \dfrac{1}{12}\right] & \text{at } |z| \leqslant \frac{c}{2}, \\ -\dfrac{\pi qc}{6s} & \text{at } |z| > \frac{c}{2}. \end{cases} \tag{2}$$

It is important that $\phi_0^{\mathrm{mod}}(z)$ is a constant at $|z| > c/2$ and so it does not affect the energy of any electrically neutral object situated in this region. Furthermore, the potential shift described by

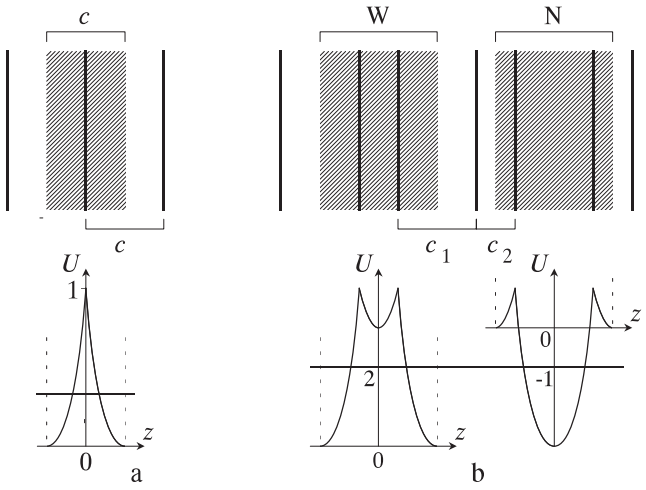

Figure 1. (a) Planes of point charges shown as heavy lines form a regular structure at the top, where a single symmetric layer is exhibited by hatching. The potential U generated by that layer and measured in units of $\pi qc/(2s)$ is shown at the bottom, where the horizontal line indicates the shift of the origin. (b) In a similar structure, but with $c_1 = 2c_2$, symmetric layers indicated by hatching have their boundaries either within wide interplanar distances (case W) or within narrow ones (case N). Their potentials U shown beneath are measured in units of $\pi qc_2^2/v$. After respective shifts, the origin is common to both the cases.

$\bar{\phi}_0$ and shown at the bottom in figure 1(a) is essential to the general potential treatment [48], but is also immaterial to the energy problem outside that layer.

Another situation we are interested in is associated with two alternating interplanar distances c_1 and c_2. The decomposition of the structure into symmetric layers containing two planes of point charges is possible in two ways leading either to case W or to case N, as shown at the top in figure 1(b). Note that now $c_1 + c_2 = c$ and a background is described by the density $\tilde{\rho} = -2q/v$, with $v = sc$. In case W the boundary-value problem is specified by functions $\phi_{01}(z)$ at $|z| \leqslant c_2/2$ and $\phi_{02}(z)$ at $c_2/2 < |z| \leqslant c/2$ which are defined by

$$\begin{aligned} &\frac{\mathrm{d}^2\phi_{0j}(z)}{\mathrm{d}z^2} = -4\pi\tilde{\rho}, \qquad \left.\frac{\mathrm{d}\phi_{01}(z)}{\mathrm{d}z}\right|_{z=0} = 0, \qquad \phi_{01}\Big(\Big|\frac{c_2}{2}\Big|\Big) = \phi_{02}\Big(\Big|\frac{c_2}{2}\Big|\Big), \\ &\left[\frac{\mathrm{d}\phi_{01}(z)}{\mathrm{d}z} - \frac{\mathrm{d}\phi_{02}(z)}{\mathrm{d}z}\right]_{z=\pm c_2/2} = \pm\frac{4\pi q}{s}, \qquad \phi_{02}\Big(\Big|\frac{c}{2}\Big|\Big) = 0. \end{aligned} \tag{3}$$

The solution is as follows:

$$\phi_{0W}^{\mathrm{mod}}(z) = \frac{\pi q}{v} \times \begin{cases} \left(4z^2 + \dfrac{3c_1^2 - c^2}{3}\right) & \text{at } 0 \leqslant |z| \leqslant \frac{c_2}{2}, \\ \left[(c - 2|z|)^2 + \dfrac{3c_2^2 - c^2}{3}\right] & \text{at } \frac{c_2}{2} \leqslant |z| \leqslant \frac{c}{2}, \\ \dfrac{3c_2^2 - c^2}{3} & \text{at } |z| > \frac{c}{2}, \end{cases} \tag{4}$$

where the mean potential $\bar{\phi}_{0W} = \pi q(c^2 - 3c_2^2)/(3v)$ is subtracted as well.

The result for case N in figure 1(b) follows from (4) after interchanging $c_1 \leftrightarrow c_2$ and is of the form

$$\phi_{0N}^{\mathrm{mod}}(z) = \frac{\pi q}{v} \times \begin{cases} \left(4z^2 + \dfrac{3c_2^2 - c^2}{3}\right) & \text{at } 0 \leqslant |z| \leqslant \frac{c_1}{2}, \\ \left[(c - 2|z|)^2 + \dfrac{3c_1^2 - c^2}{3}\right] & \text{at } \frac{c_1}{2} \leqslant |z| \leqslant \frac{c}{2}, \\ \dfrac{3c_1^2 - c^2}{3} & \text{at } |z| > \frac{c}{2}. \end{cases} \tag{5}$$

Note that results (4) and (5) are described by the same origin and so may be thought of as a continuation of each other, as depicted at the bottom in figure 1(b). Constant potential values at $|z| > c/2$ still imply that they do not contribute to the energy of any neutral object beyond either of such complex layers.

As far as the modulated part of the potential is concerned, every plane of point charges can be considered as an independent potential source. According to the translational symmetry along the plane in question, the general form of the potential generated by a single plane can be written down as

$$\phi(\mathbf{r}_\parallel, z) = \sum_{\mathbf{h}}{}' f_{\mathbf{h}}(z) \exp\bigl[2\pi \mathrm{i}(\mathbf{h}\mathbf{r}_\parallel)\bigr], \tag{6}$$

where $\mathbf{h}$ is the two-dimensional reciprocal lattice vector, the prime on the summation sign implies missing the term with $\mathbf{h} = 0$, because this term corresponds to $\phi_0(z)$ discussed above, $\mathbf{r}_\parallel$ is the two-dimensional vector along the plane specified by $\mathbf{a}_1$ and $\mathbf{a}_2$, and the expansion coefficients $f_{\mathbf{h}}(z)$ depend on the coordinate z normal to the source plane of charges, with its origin lying on that plane, and can be obtained directly as Fourier transforms of the lattice series of pair-wise Coulomb potentials [47, 49].

However, it seems to be easier to determine them as solutions of the boundary-value problem, in accord with the original approach of Madelung [50]. We start from the two-dimensional charge distribution $\sigma(\mathbf{r}_\parallel)$ in the source plane, subtracting the part uniform in $\mathbf{r}_\parallel$. Like (6), this quantity can be expanded in a series

$$\sigma(\mathbf{r}_\parallel) = \sum_{\mathbf{h}}{}' g_{\mathbf{h}} \exp\bigl[2\pi \mathrm{i}(\mathbf{h}\mathbf{r}_\parallel)\bigr], \tag{7}$$

where the prime on the summation sign means that the $\mathbf{h} = 0$ term is omitted, the structure factors $g_{\mathbf{h}}$ are defined as

$$g_{\mathbf{h}} = \frac{1}{s} \int_{\mathrm{mesh}} \sigma(\mathbf{r}_\parallel) \exp\bigl[-2\pi \mathrm{i}(\mathbf{h}\mathbf{r}_\parallel)\bigr] \mathrm{d}\mathbf{r}_\parallel, \tag{8}$$

with the integral over $\mathbf{r}_\parallel$ carried out over a unit mesh parallelogram. In the particular case of point charges q located at $\mathbf{b}_j$ within a unit mesh, relation (8) is simplified and its substitution into (7) gives rise to

$$\sigma(\mathbf{r}_\parallel) = \frac{q}{s} \sum_{\mathbf{h},j}{}' \exp\bigl[2\pi \mathrm{i}\mathbf{h}(\mathbf{r}_\parallel - \mathbf{b}_j)\bigr]. \tag{9}$$

Function (6) is then determined by Laplace's equation with the boundary condition

$$\frac{\mathrm{d}\phi(\mathbf{r}_\parallel, z)}{\mathrm{d}z}\Big|_{z=0\pm} = \mp 2\pi\sigma(\mathbf{r}_\parallel). \tag{10}$$

On integrating the equation for every particular $f_{\mathbf{h}}(z)$ in an independent manner and inserting those results into (6), the constants of integration are determined upon substituting the series obtained into (10) and comparing with the contribution of (9) there. As a result, we derive

$$\phi(\mathbf{r}_\parallel, z) = \frac{q}{s} \sum_{\mathbf{h},j}{}' \frac{\exp(-2\pi|\mathbf{h}|\,|z|)}{|\mathbf{h}|} \cos\bigl[2\pi\mathbf{h}(\mathbf{r}_\parallel - \mathbf{b}_j)\bigr], \tag{11}$$

where the exponential function of a fluctuating part is replaced by the cosine function due to the inversion symmetry of summation over **h**. Formula (11) is just the result of Sholl [47]. If we concentrate on the rectangular lattices, then for the general reciprocal lattice vector we obtain

$$\mathbf{h} = \mathbf{h}_1 l_1 + \mathbf{h}_2 l_2, \qquad |\mathbf{h}| = \left(\frac{l_1^2}{a_1^2} + \frac{l_2^2}{a_2^2} \right)^{1/2}, \tag{12}$$

where l_1 and l_2 are integers and $\mathbf{h}_\alpha = \mathbf{e}_\alpha / a_\alpha$. In this case relation (11) can be rewritten as

$$\phi(\mathbf{r}_\parallel, z) = \frac{q}{a_1 a_2} \sum_{l_1, l_2 = -\infty}^{\infty}{}' \frac{\exp(-2\pi |\mathbf{h}|\, |z|)}{|\mathbf{h}|} \sum_j \cos\left[\frac{2\pi l_1}{a_1} (r_1 - b_{j1}) \right] \cos\left[\frac{2\pi l_2}{a_2} (r_2 - b_{j2}) \right], \tag{13}$$

where the prime on the summation sign denotes missing the term with $l_1 = l_2 = 0$ and r_α and $b_{j\alpha}$ are the components of $\mathbf{r}_\parallel$ and $\mathbf{b}_j$ along $\mathbf{e}_\alpha$, respectively. It is worth noting that every cosine function in formula (11) is now represented as a product of two cosine functions [51]. The latter result can be easily obtained by direct manipulations with the series at hand, bearing in mind that all the factors, except cosine functions, depend on l_1^2 and l_2^2 and so do not change upon changing the sign of either l_1 or l_2.

3. Coulomb interaction between two semi-infinite parts of a jellium-model structure

According to the conventional standpoint [3, 5], the chief electrostatic contribution to the surface energy can be evaluated as an effect of Coulomb interaction between two semi-infinite hemi-crystals divided by a plane boundary suggested in the bulk of a perfect crystal structure. This is the reason that the interaction energy of this kind is the subject of our further investigation.

The general scheme of calculation of this energy is shown in figure 2. As mentioned above, the potential $\phi_0(z)$ created by every symmetric layer is a constant outside that layer and so does not contribute to the interaction energy characteristic of any electrically neutral portion separated by vertical lines on the right-hand side in figure 2. One more peculiarity of the jellium model is associated with the fact that the interaction of a background with the modulated part of the potential also vanishes because this contribution actually corresponds to averaging the modulated potential over a unit mesh [47]. It is interesting to note that the latter property is quite general and so independent of the mode of lattice summation [51]. Thus, the only nonzero contribution to the energy of interest is described by the effect of the modulated potential from one half of a crystal on point charges belonging to the other half, as shown in figure 2.

The structural characteristics typical of the task are naturally as follows: (i) the period c along the z axis normal to the cleavage plane in question, (ii) the number k of plane lattices of point charges per period, of which distribution along c is described by the parameters p_i with $1 \leqslant i \leqslant k$, and (iii) the orthogonal lattice parameters a_1 and a_2 of a plane lattice and the coordinates $b_{j,1}$ and $b_{j,2}$ of basis vectors $\mathbf{b}_j$ attributed to every plane lattice of summation, with a common origin on lattice 1, for definiteness. It is also convenient to represent $|z|$ in formula (13) as $|z| \Rightarrow z + z'$, in accord with figure 2. The plane-wise summation scheme can then be described in the general form

$$\begin{aligned} &z' = c(m' + p_1), \qquad z = c(m - p_1) \qquad \text{lattice } 1, \\ &\cdots \\ &z' = c(m' + p_k), \qquad z = c(m - p_k) \qquad \text{lattice } k, \end{aligned} \tag{14}$$

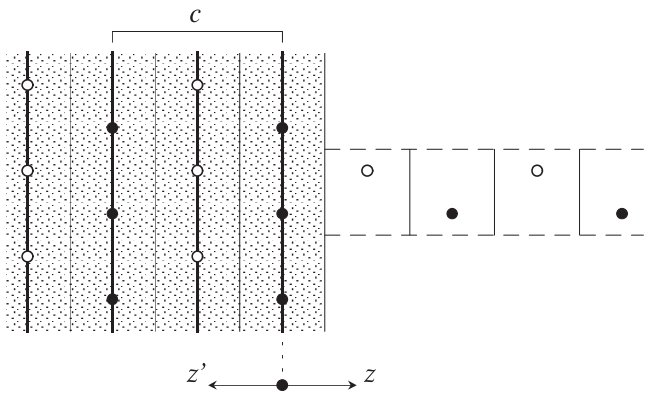

Figure 2. The scheme of calculating the energy of Coulomb interaction between two semi-infinite jellium-model hemi-crystals divided by a plane boundary. Thin vertical lines single out symmetric neutral layers, each of which contains point charges on its middle plane. In this figure two types of lattices are considered as an example, so that open circles mark point charge lattices shifted anyhow from those denoted by filled circles. The heavy vertical lines on the hatched domain exhibit such parallel planes, with the period c, summation over which along z' results in the potential as a function of z beyond the hatched domain. The energy per unit area arises as an effect of that potential on charges within the column of a unit area cross-section depicted by dashed lines on the right-hand side.

where $m' \geqslant 0$ and $m \geqslant 1$ are integer parameters of summation along the z axis. The aforementioned parameters for all the cases under consideration are compiled in the appendix, for convenience.

As a first example, we consider a simple cubic (sc) structure with the lattice spacing d and focus our attention on the cleavage plane orientation $(1, 0, 0)$ driven by relations (A.1), (A.12), (A.16) and (A.17) in the appendix. Based on (13), utilizing z' from (14) and summing over m', we obtain

$$U(\mathbf{r}_\parallel, z) = \frac{q}{d} \sum_{l_1,l_2=-\infty}^{\infty\prime} \frac{\exp\left(-\frac{2\pi L_1 z}{d}\right)\cos\left(\frac{2\pi l_1 r_1}{d}\right)\cos\left(\frac{2\pi l_2 r_2}{d}\right)}{L_1(1-F_1)}, \tag{15}$$

where

$$L_1 = \left(l_1^2 + l_2^2\right)^{-1/2}, \qquad F_1 = \exp\left(-2\pi L_1\right). \tag{16}$$

Note that throughout this paper every quantity, like L_1, under the summation sign is supposed to be a function of l_1 and l_2, but its arguments l_1 and l_2 will be omitted for brevity.

Figure 2 shows that the energy of interest arises if we multiply (15) by q at $r_1 = b_{11}$, $r_2 = b_{12}$, substitute z from (14) and carry out the summation over m. As a result, the energy per point charge is

$$\mathcal{E}^{\mathrm{sc}}_{(1,0,0)} = \frac{q^2}{d} \sum_{l_1,l_2=-\infty}^{\infty\prime} M^-(L_1, F_1), \tag{17}$$

where we introduce the characteristic functions of the general form

$$M^\pm(L, F) = \frac{F}{L(1 \pm F)^2} \tag{18}$$

and relations (16) are employed as well.

The case of the sc lattice with the $(1, 1, 0)$ cleavage plane is more complicated and is described by (A.1), (A.2), (A.13), (A.18) and (A.19) in the appendix. A novel feature is

associated with some modification of the final summation over l_1 and l_2. Indeed, taking into account the charge positions given by (A.1) and (A.2) upon summing over both m' and m, we derive

$$\mathcal{E}^{\mathrm{sc}}_{(1,1,0)} = \frac{q^2}{d} \sum_{l_1,l_2=-\infty}^{\infty\prime} \frac{F_2}{L_2(1-F_2^2)^2} \left[2F_2 + (1+F_2^2)\cos(\pi l_2)\right], \tag{19}$$

where

$$L_2 = \left(2l_1^2 + l_2^2\right)^{-1/2}, \qquad F_2 = \exp\left(-\pi L_2\right). \tag{20}$$

Keeping in mind that $\cos(\pi l_2)$ is equal to either $+1$ or -1 for l_2 even and odd, respectively, the expression in the square brackets on the right-hand side of (19) can be cast in the form

$$2F_2 + (1+F_2^2)\cos(\pi l_2) = \begin{cases} (1+F_2)^2 & l_2 \text{ even}, \\ -(1-F_2)^2 & l_2 \text{ odd}. \end{cases} \tag{21}$$

On substituting (21) into (19), we finally obtain

$$\mathcal{E}^{\mathrm{sc}}_{(1,1,0)} = \frac{q^2}{d} \left[\sum_{\substack{l_1,l_2=-\infty \\ \{l_2 \text{ even}\}}}^{\infty\prime} M^-(L_2, F_2) - \sum_{\substack{l_1,l_2=-\infty \\ \{l_2 \text{ odd}\}}}^{\infty} M^+(L_2, F_2) \right]. \tag{22}$$

4. General consideration of cubic structures

Apart from the sc structure, here we consider the body-centred (bcc), face-centred (fcc) and diamond (cd) cubic structures. The procedure of calculation is similar to that described in the previous section. The $(1, 0, 0)$ cleavage plane for bcc and fcc lattices is described by (A.1), (A.4), (A.13), (A.16) and (A.17) in the appendix. Note that the summation scheme for the $(1, 1, 0)$ cleavage plane in the case of fcc described by (A.1), (A.4), (A.18) and (A.19) turns out to be the same. As a result, we obtain

$$\left.\begin{matrix} \mathcal{E}^{\mathrm{bcc,fcc}}_{(1,0,0)} \\ \mathcal{E}^{\mathrm{fcc}}_{(1,1,0)} \end{matrix}\right\} = \frac{Dq^2}{d} \left[\sum_{\substack{l_1,l_2=-\infty \\ \{l_1+l_2 \text{ even}\}}}^{\infty\prime} M^-(L_c, F_c) - \sum_{\substack{l_1,l_2=-\infty \\ \{l_1+l_2 \text{ odd}\}}}^{\infty} M^+(L_c, F_c) \right], \tag{23}$$

where

$$\begin{array}{llll} D = 1, & L_c = L_1, & F_c = \exp(-\pi L_1) & (1,0,0) \text{ bcc}, \\ D = \sqrt{2}, & L_c = L_1, & F_c = \exp(-\pi L_1\sqrt{2}) & (1,0,0) \text{ fcc}, \\ D = \sqrt{2}, & L_c = L_2, & F_c = \exp(-\pi L_2/\sqrt{2}) & (1,1,0) \text{ fcc}, \end{array} \tag{24}$$

L_1 and L_2 are defined by (16) and (20), respectively.

Based on (A.1)–(A.4) and (A.15)–(A.17), for the $(1, 0, 0)$ cleavage plane in the cd case we easily derive

$$\mathcal{E}^{\mathrm{cd}}_{(1,0,0)} = \frac{Dq^2}{d} \left[\sum_{\substack{l_1,l_2=-\infty \\ \{l_1,l_2 \text{ even}\}}}^{\infty\prime} M^-(L_1, \hat{F}_1) - 2 \sum_{\substack{l_1,l_2=-\infty \\ \{l_1+l_2 \text{ odd}\}}}^{\infty} M^+(L_1, \tilde{F}_1) - \sum_{\substack{l_1,l_2=-\infty \\ \{l_1,l_2 \text{ odd}\}}}^{\infty} M^+(L_1, \hat{F}_1) \right], \tag{25}$$

where D and $\tilde{F}_1$ are determined by (24) in the $(1, 0, 0)$ fcc case and $\hat{F}_1 = (\tilde{F}_1)^{1/2}$.

The (1, 1, 0) cleavage plane in the bcc case is described by (A.5), (A.8), (A.13), (A.18) and (A.19) in the appendix. Utilizing these results in the summation scheme (14), the energy per point charge takes the form

$$\mathcal{E}^{\mathrm{bcc}}_{(1,1,0)} = \frac{2q^2}{d}\left[\sum_{\substack{l_1,l_2=-\infty \\ \{l_1,l_2 \text{ even}\}}}^{\infty\prime} M^-(L_2, F_2) - \sum_{\substack{l_1,l_2=-\infty \\ \{l_1,l_2 \text{ odd}\}}}^{\infty} M^+(L_2, F_2)\right], \tag{26}$$

where L_2 and F_2 are still specified by (20). Likewise, the calculation for the (1, 1, 0) cleavage plane in the cd structure is based on (A.1), (A.4), (A.9), (A.13), (A.18) and (A.19) in the appendix and yields

$$\mathcal{E}^{\mathrm{cd}}_{(1,1,0)} = \frac{q^2\sqrt{2}}{d}\left\{\sum_{\substack{l_1,l_2=-\infty \\ \{l_1,l_2 \text{ odd}\}}}^{\infty}\left[M^-(L_2, F_{\mathrm{c}}) - \sqrt{2}\,M^+(L_2, F_2)\right]\right.$$

$$\left. + \sqrt{2}\sum_{\substack{l_1,l_2=-\infty \\ \{l_1,l_2 \text{ even}\}}}^{\infty\prime} M^-(L_2, F_2) - \sum_{\substack{l_1,l_2=-\infty \\ \{l_1 \text{ even}\} \\ \{l_2 \text{ odd}\}}}^{\infty\prime} M^+(L_2, F_{\mathrm{c}})\right\}, \tag{27}$$

making use of (20) and with F_{c} defined by (24) in the (1, 1, 0) fcc case.

In the case of the (1, 1, 1)-cleavage plane orientation, every individual plane lattice is hexagonal and can be represented as a combination of two simple rectangular lattices [52]. As a result, the overall structure is described by (A.5)–(A.7) in the appendix. The corresponding structural parameters are given by (A.20)–(A.22). So, the summation in the sc, bcc and fcc cases is described by (A.14) and (A.23).

The situation is somewhat distinct if we deal with the cd structure, as shown in figure 3. The alternation in the value of interplanar spacing implies that there are two types of symmetric layers of charges responsible for the uniform potential contribution beyond these layers, as depicted in figure 1(b). In this event $c_1 = c/4$ and $c_2 = c/12$. As a result, the corresponding two types of position of the cleavage plane appear as well, though every individual plane lattice of point charges described by (A.5)–(A.7) still contributes to the modulated potential of interest in an independent manner. It is worth noting that the (1, 1, 1)N case described by (A.24) gives rise to a formula that is slightly more complicated than those for the three other structures at hand. Hence, all these cases can be written in a combined manner as

$$\left.\begin{matrix}\mathcal{E}^{\mathrm{sc,bcc,fcc}}_{(1,1,1)} \\ \mathcal{E}^{\mathrm{cd}}_{(1,1,1)\mathrm{N}}\end{matrix}\right\} = \frac{q^2 B}{d}\sum_{\substack{l_1,l_2=-\infty \\ \{l_1+l_2 \text{ even}\}}}^{\infty\prime} \frac{\tilde{F}}{L_3[1-F_3^3]^2}\left[3F_3^2 + \left(1 + 2F_3 + 2F_3^3 + F_3^4\right)\cos\frac{2\pi l_2}{3}\right], \tag{28}$$

where

$$L_3 = (3l_1^2 + l_2^2)^{1/2}, \qquad F_3 = \exp(-\pi A L_3/3), \tag{29}$$

$$\begin{aligned} &B = \sqrt{2}, \quad A = \sqrt{2} && \text{sc}, \\ &B = \sqrt{2}, \quad A = 1/\sqrt{2} && \text{bcc}, \\ &B = 2\sqrt{2}, \quad A = 2\sqrt{2} && \text{fcc, dc}, \end{aligned} \tag{30}$$

$$\tilde{F} = \begin{cases} F_3 & \text{sc, bcc, fcc}, \\ \tilde{F}_{31}(1 + \tilde{F}_{32})^2 & \text{cd}, \end{cases} \tag{31}$$

$\tilde{F}_{31} = \exp(-\sqrt{2}\pi L_3/6)$ and $\tilde{F}_{32} = \tilde{F}_{31}^3$.

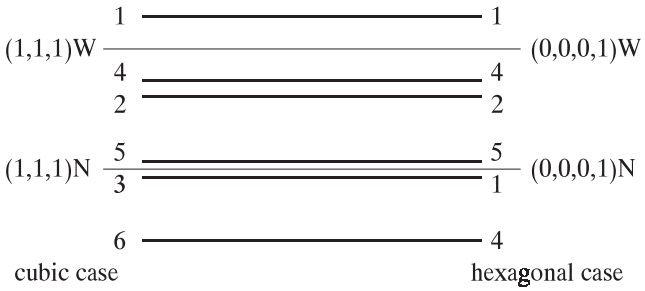

Figure 3. Diamond structures in terms of hexagonal planes shown by heavy horizontal lines, where the notations on the left and on the right correspond to the cubic and hexagonal diamond, respectively. Plane 4 arises from plane 1 by its parallel shift and the same connection is between planes 2 and 5 and between planes 3 and 6. The cleavage planes shown by thin lines and designated properly may be situated midway either within a wider interplanar distance (case W) or within a narrower one (case N).

On the other hand, case W presented in figure 3 is described by (A.25), so that the expression for the corresponding energy takes the form

$$\mathcal{E}^{\mathrm{cd}}_{(1,1,1)\mathrm{W}} = \frac{2\sqrt{2}\,q^2}{d} \sum_{\substack{l_1,l_2=-\infty \\ \{l_1+l_2 \text{ even}\}}}{}' \frac{\tilde{F}_{32}}{L_3[1-F_3^3]^2} \Big\{ \big(1+\tilde{F}_{32}^3\big)^2 + 2\tilde{F}_{32}^2\big(1+\tilde{F}_{32}\big)^2 + \tilde{F}_{31}\big(1+\tilde{F}_{32}\big) \times \Big[2\big(1+F_3\big)\big(1+\tilde{F}_{32}^3\big) + \tilde{F}_{31}\big(1+F_3^2\big)\big(1+\tilde{F}_{32}\big)\Big] \cos\frac{2\pi l_2}{3} \Big\}. \tag{32}$$

5. Energy peculiarities of hexagonal structures

Here we also consider three basic hexagonal structures whose peculiar structural features are exhibited in figure 4. A simple hexagonal (sh) structure shown in figure 4(a) will be discussed in the particular case of $|\mathbf{d}_4| = d$ so that the nearest-neighbour distances in hexagonal planes and between such planes coincide. On the other hand, interested in hexagonal close-packed (hcp) and hexagonal diamond (hd) structures, we restrict ourselves to the ideal ratio $|\mathbf{d}_4|/d = \sqrt{8/3}$. Although the latter case is not energetically favourable, at least for hcp structures, the actual deviation is negligible [45, 47]. On the other hand, this case admits a direct comparison with results for cubic structures with close structural motifs pointed out in figure 3.

We begin with the $(0, 0, 0, 1)$ orientation of the cleavage plane. According to the foregoing choice of structural parameters, the sh structure is described by (A.5), (A.12), (A.32) and (A.33), leading to

$$\mathcal{E}^{\mathrm{sh}}_{(0,0,0,1)} = \frac{2q^2}{d} \sum_{\substack{l_1,l_2=-\infty \\ \{l_1+l_2 \text{ even}\}}}{}' M^-(L_3, F_{3\mathrm{h}}), \tag{33}$$

where L_3 is defined by (29) and $F_{3\mathrm{h}} = \exp\big(-2\pi L_3/\sqrt{3}\big)$.

The hcp case is determined by (A.5), (A.6), (A.13), (A.32) and (A.34). The hd case follows from this set, where (A.13) and (A.34) must be replaced either by (A.35) or by (A.36) in cases

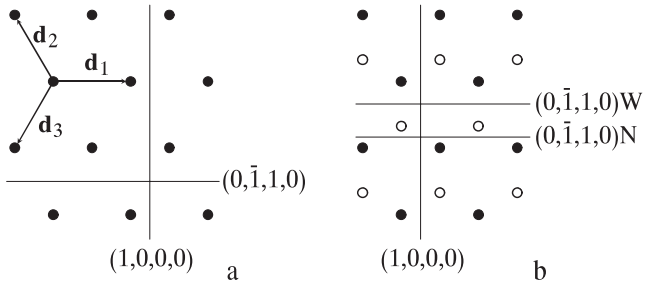

Figure 4. (a) Hexagonal plane of a simple hexagonal (sh) structure, where $\mathbf{d}_1$, $\mathbf{d}_2$ and $\mathbf{d}_3$ are typical vectors of elementary in-plane translations, with $|\mathbf{d}_1| = |\mathbf{d}_2| = |\mathbf{d}_3| = d$ and with the fourth translation vector $\mathbf{d}_4$ normal to the plane of the figure. In terms of these vectors the hexagonal plane is specified as a (0, 0, 0, 1) one, whereas two other basic planes of interest are denoted as (1, 0, 0, 0) and (0, $\bar{1}$, 1, 0) and shown by thin lines, respectively. (b) Apart from plane lattice 1 shown by filled circles, the hcp structure contains lattice 2 shown by open circles and shifted by $\mathbf{d}_4/2$ from the plane of lattice 1. So, there are two types of symmetric cleavage planes (0, $\bar{1}$, 1, 0)W and (0, $\bar{1}$, 1, 0)N midway in wider and narrower interplanar intervals, respectively.

N and W, respectively. As a result, we obtain

$$\left.\begin{matrix}\mathcal{E}^{\mathrm{hcp}}_{(0,0,0,1)}\\ \mathcal{E}^{\mathrm{hd}}_{(0,0,0,1)\mathrm{N}}\end{matrix}\right\} = \frac{2q^2}{d}\sum_{\substack{l_1,l_2=-\infty\\ \{l_1+l_2\ \text{even}\}}}^{\infty\prime}\frac{\tilde{F}\left[2F_3+\left(1+F_3^2\right)\cos\left(2\pi l_2/3\right)\right]}{L_3(1-F_3^2)^2}, \tag{34}$$

where

$$\tilde{F} = \begin{cases} F_3 & \mathrm{hcp},\\ \tilde{F}_{33}(1+\tilde{F}_{33}^3)^2 & \mathrm{hd}, \end{cases} \tag{35}$$

$F_3 = \exp(-2\sqrt{2}\pi L_3)$ and $\tilde{F}_{33}^4 = F_3$. Likewise,

$$\mathcal{E}^{\mathrm{hd}}_{(0,0,0,1)\mathrm{W}} = \frac{2q^2}{d}\sum_{\substack{l_1,l_2=-\infty\\ \{l_1+l_2\ \text{even}\}}}^{\infty\prime}\frac{\tilde{F}_{33}^3}{L_3(1-F_3^2)^2}\left[\left(1+F_3^2\right)\left(1+\tilde{F}_{33}^2\right)\right.$$
$$\left.+\,4\tilde{F}_{33}^5+2\tilde{F}_{33}\left(1+\tilde{F}_{33}^3\right)\left(1+\tilde{F}_{33}^5\right)\cos\frac{2\pi l_2}{3}\right]. \tag{36}$$

The sh structure is described by (A.1), (A.2), (A.13), (A.26) and (A.27) for the (1, 0, 0, 0) cleavage plane, but (A.26) and (A.27) must be replaced by (A.28) and (A.29) for the (0, $\bar{1}$, 1, 0) plane. Then the corresponding energy values are as follows:

$$\mathcal{E}^{\mathrm{sh}}_{\substack{(1,0,0,0)\\(0,\bar{1},1,0)}} = \frac{q^2}{d}\left[\sum_{\substack{l_1,l_2=-\infty\\ \{l_2\ \text{even}\}}}^{\infty\prime} M^-(L_\mathrm{h},F_\mathrm{h}) - \sum_{\substack{l_1,l_2=-\infty\\ \{l_2\ \text{odd}\}}}^{\infty} M^+(L_\mathrm{h},F_\mathrm{h})\right], \tag{37}$$

where

$$\begin{matrix} L_\mathrm{h}=L_3, & F_\mathrm{h}=\exp\left(-\pi L_3/\sqrt{3}\right) & (1,0,0,0),\\ L_\mathrm{h}=L_1, & F_\mathrm{h}=\exp\left(-\pi\sqrt{3}L_1\right) & (0,\bar{1},1,0), \end{matrix} \tag{38}$$

with L_1 and L_3 defined by (16) and (29), respectively.

The $(1, 0, 0, 0)$ case for the hcp and hd structures is described by (A.11), (A.13), (A.26) and (A.27). The resulting energies can also be written in a combined manner:

$$\mathcal{E}^{\mathrm{hcp,hd}}_{(1,0,0,0)} = \frac{q^2\sqrt{3}}{d}\left[\sum_{\substack{l_1,l_2=-\infty \\ \{l_1,l_2\ \text{even}\}}}^{\infty\prime} GK^+M^-(L_4, F_4) + \sum_{\substack{l_1,l_2=-\infty \\ \{l_1\ \text{even}\} \\ \{l_2\ \text{odd}\}}}^{\infty} GK^-M^-(L_4, F_4)\right.$$

$$\left. - \sum_{\substack{l_1,l_2=-\infty \\ \{l_1\ \text{odd}\} \\ \{l_2\ \text{even}\}}}^{\infty} GK^+M^+(L_4, F_4) - \sum_{\substack{l_1,l_2=-\infty \\ \{l_1,l_2\ \text{odd}\}}}^{\infty} GK^-M^+(L_4, F_4)\right], \tag{39}$$

where

$$L_4 = \left(8l_1^2 + 9l_2^2\right)^{1/2}, \qquad F_4 = \exp\left[-\pi L_4/(2\sqrt{6})\right], \tag{40}$$

$$K^{\pm} = 1 \pm \cos(2\pi l_1/3), \qquad G = \begin{cases} 1 & \text{hcp}, \\ 1 + \cos(3\pi l_2/4) & \text{hd}. \end{cases} \tag{41}$$

In the case of the $(0, \bar{1}, 1, 0)$ cleavage plane results (A.1)–(A.4) and (A.28) are relevant to hcp lattices, but they are to be modified by (A.10) for hd structures. The two possibilities typical of the case and shown in figure 4(b) are driven by (A.30) and (A.31). As a result, one can show that

$$\mathcal{E}^{\mathrm{hcp,hd}}_{(0,\bar{1},1,0)\mathrm{N}} = \frac{q^2\sqrt{3}}{d}\left[\sum_{\substack{l_1,l_2=-\infty \\ \{l_1,l_2\ \text{even}\}}}^{\infty\prime} \frac{F_{\mathrm{h}1}(1+F_{\mathrm{h}2})^2 G}{L_5(1-F_{\mathrm{h}3})^2} - \sum_{\substack{l_1,l_2=-\infty \\ \{l_1\ \text{even}\} \\ \{l_2\ \text{odd}\}}}^{\infty} \frac{F_{\mathrm{h}1}(1-F_{\mathrm{h}2})^2 G}{L_5(1-F_{\mathrm{h}3})^2}\right.$$

$$\left. - \sum_{\substack{l_1,l_2=-\infty \\ \{l_1\ \text{odd}\} \\ \{l_2\ \text{even}\}}}^{\infty} \frac{F_{\mathrm{h}1}(1+F_{\mathrm{h}2})^2 G}{L_5(1+F_{\mathrm{h}3})^2} + \sum_{\substack{l_1,l_2=-\infty \\ \{l_1,l_2\ \text{odd}\}}}^{\infty} \frac{F_{\mathrm{h}1}(1-F_{\mathrm{h}2})^2 G}{L_5(1+F_{\mathrm{h}3})^2}\right], \tag{42}$$

where G is still determined by (41),

$$L_5 = \left(8l_1^2 + 3l_2^2\right)^{1/2}, \qquad F_{\mathrm{h}1} = \exp\left[-\pi L_5/(2\sqrt{6})\right],$$
$$F_{\mathrm{h}2} = F_{\mathrm{h}1}^2, \qquad F_{\mathrm{h}3} = F_{\mathrm{h}1}^3. \tag{43}$$

In case W, the interaction energy in terms of the aforementioned notations takes the form

$$\mathcal{E}^{\mathrm{hcp,hd}}_{(0,\bar{1},1,0)\mathrm{W}} = \frac{q^2\sqrt{3}}{d}\left[\sum_{\substack{l_1,l_2=-\infty \\ \{l_1,l_2\ \text{even}\}}}^{\infty\prime} \frac{F_{\mathrm{h}2}(1+F_{\mathrm{h}1})^2 G}{L_5(1-F_{\mathrm{h}3})^2} - \sum_{\substack{l_1,l_2=-\infty \\ \{l_1\ \text{even}\} \\ \{l_2\ \text{odd}\}}}^{\infty} \frac{F_{\mathrm{h}2}(1-F_{\mathrm{h}1})^2 G}{L_5(1-F_{\mathrm{h}3})^2}\right.$$

$$\left. + \sum_{\substack{l_1,l_2=-\infty \\ \{l_1\ \text{odd}\} \\ \{l_2\ \text{even}\}}}^{\infty} \frac{F_{\mathrm{h}2}(1-F_{\mathrm{h}1})^2 G}{L_5(1+F_{\mathrm{h}3})^2} - \sum_{\substack{l_1,l_2=-\infty \\ \{l_1,l_2\ \text{odd}\}}}^{\infty} \frac{F_{\mathrm{h}2}(1+F_{\mathrm{h}1})^2 G}{L_5(1+F_{\mathrm{h}3})^2}\right]. \tag{44}$$

6. Discussion

The general feature common to all the results obtained above is the very high rate of convergence of the two-dimensional series. This property is typical of the Madelung treatment [50], that turns out to be much more effective than the widespread Ewald approach [1, 5], at least in the task at hand. As a result, the numerical values associated with formulae (17), (22), (23), (25)–(28), (32)–(34), (36), (37), (39), (42) and (44) can be immediately calculated and are listed in table 1 as values of $\mathcal{E}_1$ measured in units of q^2/d. Note that the value $\mathcal{E}_1$ is the interaction energy between two semi-infinite hemi-crystals per point charge on the surface dividing these parts. It implies that the Coulomb contribution of the modulated potential to the surface energy can be evaluated as [3, 5]

$$\mathcal{E}_{\mathrm{surf}}^{\mathrm{modul}} = -\mathcal{E}_1/2. \tag{45}$$

Another principal possibility of representation of the result is associated with the energy units q^2/r_s characteristic of the description of metals [45, 51], where $4\pi r_s^3/3 = v$. Keeping in

Table 1. The energy of Coulomb interaction between two semi-infinite hemi-crystals in a jellium model, with point charges q forming one of four cubic or three hexagonal structures, in dependence on the orientation of the cleavage plane. The energy per point charge on the interface is represented either as $\mathcal{E}_1$ measured in units of q^2/d or as $\mathcal{E}_2$, in units of q^2/r_s, where $4\pi r_s^3/3 = v$. The energy surface density E, in units of q^2/v, arises from this by means of formula (48).

Structure	Plane	$\mathcal{E}_1$ (q^2/d)	$\mathcal{E}_2$ (q^2/r_s)	E (q^2/v)
Simple cubic	(1, 0, 0)[a]	0.007 899 00	0.004 900 15	−0.003 949 50[b]
	(1, 1, 0)	−0.069 763 70	−0.043 277 95	0.024 665 19
	(1, 1, 1)	−0.107 981 51	−0.066 986 38	0.031 171 58
Body-centred cubic	(1, 0, 0)	−0.124 009 38	−0.061 058 81	0.031 002 35[b]
	(1, 1, 0)	−0.015 925 38	−0.007 841 22	0.005 630 47[b]
	(1, 1, 1)	−0.432 472 87	−0.212 937 75	0.062 422 08
Face-centred cubic	(1, 0, 0)	−0.057 347 47	−0.022 411 18	0.014 336 87[b]
	(1, 1, 0)	−0.249 269 50	−0.097 413 60	0.044 065 04[b]
	(1, 1, 1)	−0.011 253 05	−0.004 397 65	0.003 248 47[b]
Cubic diamond	(1, 0, 0)	−0.254 502 32	−0.078 940 32	0.031 812 79
	(1, 1, 0)	−0.195 431 18	−0.060 617 91	0.034 547 68
	(1, 1, 1) N	−0.755 125 99	−0.234 221 39	0.108 993 05
	(1, 1, 1)W[a]	0.077 360 64	0.023 995 36	−0.011 166 05
Simple hexagonal[c]	(1, 0, 0, 0)	−0.200 663 16	−0.118 653 80	0.050 165 79
	(0, $\bar{1}$, 1, 0)	−0.001 097 65	−0.000 649 05	0.000 475 30
	(0, 0, 0, 1)[a]	0.004 258 55	0.002 518 12	−0.002 129 28
Hexagonal close packed[d]	(1, 0, 0, 0)	−0.179 039 87	−0.098 949 87	0.044 759 97
	(0, $\bar{1}$, 1, 0)N	−0.506 288 50	−0.279 810 19	0.109 614 68
	(0, $\bar{1}$, 1, 0)W	−0.101 666 85	−0.056 188 16	0.022 011 52
	(0, 0, 0, 1)	−0.007 828 83	−0.004 326 75	0.003 196 11
Hexagonal diamond[d]	(1, 0, 0, 0)	−0.158 267 93	−0.069 424 86	0.039 566 98
	(0, $\bar{1}$, 1, 0)N	−0.458 312 97	−0.201 040 83	0.099 227 67
	(0, $\bar{1}$, 1, 0)W[a]	0.021 031 23	0.009 225 43	−0.004 553 39
	(0, 0, 0, 1)N	−0.522 787 24	−0.229 322 74	0.106 713 50
	(0, 0, 0, 1)W[a]	0.060 408 47	0.026 498 42	−0.012 330 83

[a] The instability is typical of this case.
[b] This value agrees with the result quoted in [5].
[c] The ratio $|\mathbf{d}_4|/d = 1$ is suggested.
[d] The ideal ratio $|\mathbf{d}_4|/d = \sqrt{8/3}$ is suggested.

Table 2. The values of α connecting E and $\mathcal{E}_1$ by means of (48) in dependence on the structure and cleavage plane orientation.

	(1, 0, 0)	(1, 1, 0)	(1, 1, 1)		(1, 0, 0, 0)	(0, $\bar{1}$, 1, 0)	(0, 0, 0, 1)
sc	$-1/2$	$-1/\sqrt{8}$	$-1/\sqrt{12}$	sh	$-1/4$	$-\sqrt{3}/4$	$-1/2$
bcc	$-1/4$	$-1/\sqrt{8}$	$-1/\sqrt{48}$	hcp	$-1/4$	$-\sqrt{3}/8$	$-1/\sqrt{6}$
fcc	$-1/4$	$-1/\sqrt{32}$	$-1/\sqrt{12}$	hd	$-1/4$	$-\sqrt{3}/8$	$-1/\sqrt{24}$
cd	$-1/8$	$-1/\sqrt{32}$	$-1/\sqrt{48}$				

mind that $v = d^3/n$, where $n = 1, 2, 4$ and 8 for the sc, bcc, fcc and cd structures, respectively, we readily obtain

$$\frac{1}{d} = \left(\frac{3}{4\pi n}\right)^{1/3} \frac{1}{r_s} \tag{46}$$

for all cubic cases. One can also show that $v = d^3\sqrt{3}/2$ for the sh structure at hand, but $v = d^3/(m\sqrt{2})$, with $m = 1$ and 2 for the ideal hcp and hd structures, respectively. Then we derive

$$\frac{1}{d} = \frac{1}{r_s} \times \begin{cases} \left(\dfrac{\sqrt{27}}{8\pi}\right)^{1/3} & \text{sh,} \\ \left(\dfrac{3}{4\sqrt{2}\,\pi m}\right)^{1/3} & \text{hcp, hd.} \end{cases} \tag{47}$$

The corresponding energy denoted as $\mathcal{E}_2$ is given in table 1. Relation (45) is naturally extended to $\mathcal{E}_2$ as well.

The representation of the above results in terms of the two-dimensional density of the Coulomb part of the surface energy is also expedient. Measured in units of q^2/v, where v is the volume per point charge, the corresponding quantity E is quite suitable for the problem of self-consistent description of electron states near the surface [5]. On the other hand, the product Es is equal to $\mathcal{E}_{\text{surf}}^{\text{modul}}$ given by (45), where s is the area per point charge in the plane of interest. Keeping in mind that $\mathcal{E}_1$ is measured in units of q^2/d, one can show that

$$E = -\frac{v}{2sd}\mathcal{E}_1 \equiv \alpha\mathcal{E}_1. \tag{48}$$

For convenience, the values of α in the particular cases under consideration are compiled in table 2. Making use of these results, the corresponding values of E are readily obtained and are shown in table 1 as well.

It is worth noting that the most symmetric orientations of the cleavage plane are considered. As anticipated, both the limiting values bounding the energy of interest for each structure at hand are thus obtained. Our estimates for the sc, bcc and fcc lattices agree with the known results [5]. The only exception is associated with the (1, 1, 1) bcc case, where our result turns out to be almost twice as large. Presumably, a normalization parameter distinct from that in table 2 was employed in [5].

Table 1 shows that there are cases with positive values of $\mathcal{E}_1$. For the sc structure such a result was obtained earlier [5]. We have obtained that the same situation is typical of the simple hexagonal and both diamond structures. It implies that the instability associated with the tendency towards splitting of all emphasized structures in a spontaneous manner must be expected. As a result, we draw a conclusion that the jellium model, at least in its simplest form, is not principally applicable to these structures. As far as the diamond structures are concerned, it is interesting to note that the structural motif common to both of these structures and shown

in figure 3 results in the chief planes of instability. Indeed, the unstable hexagonal (1, 1, 1)W plane in the cd structure evidently corresponds to the (0, 0, 0, 1)W plane in the hd structure.

As for the other three structures, all the energies of Coulomb interaction discussed are negative and so describe the attraction. It is evident that a maximum energy in each case specifies the most favourable plane of cleavage. It appears that it is the (1, 1, 0) plane in the bcc structure, the hexagonal (1, 1, 1) plane in the fcc structure and the hexagonal (0, 0, 0, 1) plane in the hcp structure. Note that all these cases correspond to the highest two-dimensional densities of point charges in the planes at hand, in accord with table 2.

7. Conclusion

The plane-wise summation is employed for calculating the energy of Coulomb interaction between two semi-infinite parts of a crystal divided by a cleavage plane in a jellium model. The classical treatment of the uniform potential contribution is extended to alternating interplanar distances. As a result, we have shown that any layer separated as an individual potential source can be defined in a symmetric manner and so it does not function as a double layer disturbing the translational symmetry.

The modulated part of the potential generated by a plane lattice of equal point charges is derived within the original approach of Madelung, that turns out to be much simpler than the known treatment of Sholl. Four cubic structures, simple, body centred, face centred and diamond, are considered along with three hexagonal structures, simple, close packed and diamond. Three fundamental orientations of the cleavage plane are examined in each case mentioned above. As a result, 25 basic formulae for the interaction energy of interest have been obtained. Note that their extension to cases of lower symmetry is straightforward.

The numerical calculation based on these formulae is very effective and is readily performed. As a result, we have shown that the four structures, simple and diamond in both the cubic and hexagonal cases, are characterized by positive values of the interaction energy and so they are expected to be unstable with respect to their spontaneous cleavage. To our mind, this fact prevents the application of a jellium model to these structures.

As far as the other three stable structures are concerned, we have shown that the orientation of their energetically favourable cleavage corresponds to planes with the highest two-dimensional density of point charges.

Acknowledgment

We are grateful to Professor N K Moroz for interesting discussions concerning this work.

Appendix. Parameters of the plane-wise summation scheme in the cases under consideration

There are typical basis vectors describing plane lattices in terms of lattice constants a_1 and a_2. In the case of simple lattice species, we define

$$b_{11} = b_{12} = 0 \qquad \text{lattice 1,} \tag{A.1}$$

$$b_{21} = 0, \qquad b_{22} = a_2/2 \qquad \text{lattice 2,} \tag{A.2}$$

$$b_{31} = a_1/2, \qquad b_{32} = 0 \qquad \text{lattice 3,} \tag{A.3}$$

$$b_{41} = a_2/2, \qquad b_{42} = a_2/2 \qquad \text{lattice 4,} \tag{A.4}$$

where (A.1) can also be treated as a reference point common to all the lattices discussed together. If every plane lattice may be treated as a combination of two simple ones, then the typical cases of such lattices are of the form

$$b_{11} = b_{12} = 0, \qquad b_{21} = a_1/2, \quad b_{22} = a_2/2 \qquad \text{lattice 1(4)}, \tag{A.5}$$

$$b_{31} = 0, \quad b_{32} = -a_2/3, \quad b_{41} = a_1/2, \quad b_{42} = a_2/6 \qquad \text{lattice 2(5)}, \tag{A.6}$$

$$b_{51} = 0, \quad b_{52} = a_2/3, \quad b_{61} = a_1/2, \quad b_{62} = -a_2/6 \qquad \text{lattice 3(6)}, \tag{A.7}$$

$$b_{71} = 0, \quad b_{72} = a_2/2, \quad b_{81} = a_1/2, \quad b_{82} = 0 \qquad \text{lattice 7}. \tag{A.8}$$

Another case of interest appears when lattices (A.1) and (A.4) are modified by the following sublattices:

$$\begin{array}{llll} b_{51} = a_1/2, & b_{52} = a_2/4 & \text{lattice 1}, \\ b_{61} = 0, & b_{62} = -a_2/4 & \text{lattice 4}. \end{array} \tag{A.9}$$

One more case is associated with the modification of the total set (A.1)–(A.4) by the sublattices of the form

$$\begin{array}{llll} b_{51} = 0, & b_{52} = -3a_2/8 & \text{lattice 1}, \\ b_{61} = 0, & b_{62} = a_2/8 & \text{lattice 2}, \\ b_{71} = a_1/2, & b_{72} = -3a_2/8 & \text{lattice 3}, \\ b_{81} = a_1/2, & b_{82} = a_2/8 & \text{lattice 4}. \end{array} \tag{A.10}$$

There is also a special case described by

$$\begin{array}{llll} b_{11} = b_{12} = 0, & b_{21} = a_1/3, & b_{22} = a_2/2, & \left.\begin{array}{l}\\\end{array}\right\} \text{lattice 1}, \\ b_{31} = 0, \quad b_{32} = 3a_2/8, & b_{41} = a_1/3, & b_{42} = -a_2/8 & \\ b_{51} = a_1/2, \quad b_{52} = 0, & b_{61} = -a_1/6, & b_{62} = a_2/2, & \left.\begin{array}{l}\\\end{array}\right\} \text{lattice 2}. \\ b_{71} = a_1/2, \quad b_{72} = 3a_2/8, & b_{81} = -a_1/6, & b_{82} = -a_2/8 & \end{array} \tag{A.11}$$

There are four typical cases of lattices distributed evenly and described by

$$k = 1: \quad p_{j_1} = 0, \tag{A.12}$$

$$k = 2: \quad p_{j_1} = 0, \quad p_{j_2} = 1/2, \tag{A.13}$$

$$k = 3: \quad p_{j_1} = 0, \quad p_{j_2} = 1/3, \quad p_{j_3} = 2/3, \tag{A.14}$$

$$k = 4: \quad p_{j_1} = 0, \quad p_{j_2} = 1/4, \quad p_{j_3} = 1/2, \quad p_{j_4} = 3/4, \tag{A.15}$$

where j_l are the numbers of the lattices mentioned above. When lattice sequences are not equidistant, those cases of interest will be described in due course.

Now we consider simple (sc), body-centred (bcc), face-centred (fcc) and diamond (cd) cubic structures with the lattice spacing d. The (1, 0, 0) cleavage plane is then described by

$$c = d, \qquad a_1 = a_2 = \begin{cases} d & \text{sc, bcc}, \\ d/\sqrt{2} & \text{fcc, cd}. \end{cases} \tag{A.16}$$

The summation scheme appropriate to the case is determined by

$$\begin{array}{llll} k = 1, & j_1 = 1 & & \text{sc}, \\ k = 2, & j_1 = 1, \quad j_2 = 4, & & \text{bcc, fcc}, \\ k = 4, & j_1 = 1, \quad j_2 = 3, \quad j_3 = 4, & j_4 = 2 & \text{cd}, \end{array} \tag{A.17}$$

providing that lattices (A.1)–(A.4) are taken into account with their proper numbers there.

The (1, 1, 0) cleavage plane is determined by

$$\begin{array}{ll} a_1 = d, \quad a_2 = c = d\sqrt{2} & \text{sc, bcc}, \\ a_2 = d, \quad a_1 = c = d/\sqrt{2} & \text{fcc, cd}, \end{array} \tag{A.18}$$

$$\begin{array}{l} k = 2, \quad j_1 = 1, \\ j_2 = 2 \quad \text{(sc)}, \quad \text{or} \quad j_2 = 4 \quad \text{(fcc, cd)}, \quad \text{or} \quad j_2 = 7 \quad \text{(bcc)}, \end{array} \tag{A.19}$$

where (A.1), (A.2) and (A.4) are utilized in the first two cases associated with j_2 in formula (A.19), providing that those lattices are modified by (A.9) in the cd case. On the other hand, (A.5) and (A.8) are to be employed for the bcc case.

Likewise, for the (1, 1, 1) cleavage plane we obtain

$$a_1 = d\sqrt{2}, \quad a_2 = d\sqrt{6}, \quad c = d\sqrt{3} \quad \text{sc}, \tag{A.20}$$

$$a_1 = d\sqrt{2}, \quad a_2 = d\sqrt{6}, \quad c = d\sqrt{3}/2 \quad \text{bcc}, \tag{A.21}$$

$$a_1 = d/\sqrt{2}, \quad a_2 = d\sqrt{3/2}, \quad c = d\sqrt{3} \quad \text{fcc, cd}, \tag{A.22}$$

$$k = 3, \quad j_1 = 1, \quad j_2 = 2, \quad j_3 = 3 \quad \text{sc, bcc, fcc}, \tag{A.23}$$

On the other hand, there are two possibilities in the cd case, as shown in figure 3. In both these events $k = 6$, but

$$\begin{aligned} &p_1 = 0, \quad p_2 = 1/3, \quad p_3 = 2/3, \\ &p_4 = 1/4, \quad p_5 = 7/12, \quad p_6 = 11/12 \quad \text{case cd (1, 1, 1)N}, \end{aligned} \tag{A.24}$$

$$\begin{aligned} &p_1 = 3/4, \quad p_2 = 1/12, \quad p_3 = 5/12, \\ &p_4 = 0, \quad p_5 = 1/3, \quad p_6 = 2/3 \quad \text{case cd (1, 1, 1)W}. \end{aligned} \tag{A.25}$$

Note that in formulae (A.23)–(A.25) the lattices are defined by (A.5)–(A.7) with their proper numbers as well.

Now we consider hexagonal lattices: simple (sh), close-packed (hcp) and diamond (hd) ones. The (1, 0, 0, 0) cleavage plane shown in figure 4 is described by

$$\begin{aligned} &a_1 = c = d, \quad a_2 = d\sqrt{3} \quad \text{sh}, \\ &a_1 = d\sqrt{3}, \quad a_2 = d\sqrt{8/3}, \quad c = d \quad \text{hcp, hd}, \end{aligned} \tag{A.26}$$

$$k = 2, \quad j_1 = 1, \quad j_2 = 2 \tag{A.27}$$

where (A.1) and (A.2) correspond to the sh case and (A.11) is relevant to the hd case, but only the first lines of the parameters for either lattice are essential to the hcp case there.

The $(0, \bar{1}, 1, 0)$ cleavage plane shown in figure 4 is described by

$$\begin{aligned} &a_1 = a_2 = d, \quad c = d\sqrt{3} \quad \text{sh}, \\ &a_1 = d, \quad a_2 = d\sqrt{8/3}, \quad c = d\sqrt{3} \quad \text{hcp, hd}, \end{aligned} \tag{A.28}$$

$$k = 2, \quad j_1 = 1, \quad j_2 = 2 \quad \text{sh}, \tag{A.29}$$

where (A.1) and (A.2) correspond to the sh case again. The hcp case is described by (A.1)–(A.4), which are modified by (A.10) in the hd case. Moreover, the N and W possibilities are typical of both these cases, as depicted in figure 4. In these events $k = 4$ and, instead of (A.15), the shift parameters are of the form

$$p_1 = 0, \quad p_2 = 1/3, \quad p_3 = 1/2, \quad p_4 = 5/6 \quad \text{case N}, \tag{A.30}$$

$$p_1 = 2/3, \quad p_2 = 0, \quad p_3 = 1/6, \quad p_4 = 1/2 \quad \text{case W}. \tag{A.31}$$

Finally, the (0, 0, 0, 1) cleavage plane is determined by

$$\begin{aligned} &a_1 = c = d, \quad a_2 = d\sqrt{3} \quad \text{sh}, \\ &a_1 = d, \quad a_2 = d\sqrt{3}, \quad c = d\sqrt{8/3} \quad \text{hcp, hd}, \end{aligned} \tag{A.32}$$

$$k = 1, \quad j_1 = 1, \quad \text{sh}, \tag{A.33}$$

$$k = 2, \quad j_1 = 1, \quad j_2 = 2 \quad \text{hcp}, \tag{A.34}$$

where (A.5) specifies the sh case, but (A.5) and (A.6) are inherent in the hcp and hd cases. However, figure 4 shows that there are N and W possibilities in the latter case as well. It implies that $k = 4$ for hd lattices and

$$p_1 = 0, \quad p_2 = 1/2, \quad p_4 = 3/8, \quad p_5 = 7/8 \quad \text{case N}, \tag{A.35}$$

$$p_1 = 5/8, \quad p_2 = 1/8, \quad p_4 = 0, \quad p_5 = 1/2 \quad \text{case W}. \tag{A.36}$$

References

[1] Ewald P P 1921 *Ann. Phys.* **64** 253
[2] Hund F 1935 *Z. Phys.* **94** 11
[3] Tosi M P 1964 *Solid State Physics* vol 16, ed F Seitz and D Turnbull (New York: Academic) pp 1–120
[4] Fuchs K 1935 *Proc. R. Soc.* A **151** 585
[5] Lang N D and Kohn W 1970 *Phys. Rev.* B **1** 4555
[6] Lang N D and Kohn W 1971 *Phys. Rev.* B **3** 1251
[7] Kholopov E V 2004 *Usp. Fiz. Nauk* **174** 1033 and references therein
Kholopov E V 2004 *Phys. Usp.* **47** 965 (Engl. Transl.)
[8] Perdew J P, Tran H Q and Smith E D 1990 *Phys. Rev.* B **42** 11627
[9] Shore H B and Rose J H 1999 *Phys. Rev.* B **59** 10485
[10] Doll K, Harrison N M and Saunders V R 1999 *J. Phys.: Condens. Matter* **11** 5007
[11] Sánchez-Friera P and Godby R W 2000 *Phys. Rev. Lett.* **85** 5611
[12] Alchagirov A B, Perdew J P, Boettger J C, Albers R C and Fiolhais C 2001 *Phys. Rev.* B **63** 224115
[13] Wachowicz E and Kiejna A 2001 *J. Phys.: Condens. Matter* **13** 10767
[14] Gaudoin R, Foulkes W M C and Rajagopal G 2002 *J. Phys.: Condens. Matter* **14** 8787
[15] Bonev S A and Ashcroft N W 2001 *Phys. Rev.* B **64** 224112
[16] Zhao J L, Zhang W, Li X M, Feng J W and Shi X 2006 *J. Phys.: Condens. Matter* **18** 1495
[17] Kandavel M and Ramaprabhu S 2003 *J. Phys.: Condens. Matter* **15** 7501
[18] Ohba N, Aoki M, Noritake T, Miwa K and Towata S I 2005 *Phys. Rev.* B **72** 075104
[19] Ledovskikh A, Danilov D, Rey W J J and Notten P H L 2006 *Phys. Rev.* B **73** 014106
[20] Dobson J F, Wang J and Gould T 2002 *Phys. Rev.* B **66** 081108
[21] Boettger J C 1996 *Phys. Rev.* B **53** 13133
[22] Wojciechowski K F 1999 *Phys. Rev.* B **60** 9202
[23] Thumm U, Kürpick P and Wille U 2000 *Phys. Rev.* B **61** 3067
[24] Sarria I, Henriques C, Fiolhais C and Pitarke J M 2000 *Phys. Rev.* B **62** 1699
[25] Ciraci S, Buldum A and Batra I P 2001 *J. Phys.: Condens. Matter* **13** R537
[26] Ogando E, Zabala N, Chulkov E V and Puska M J 2004 *Phys. Rev.* B **69** 153410
[27] Orosz L 1988 *Phys. Rev.* B **37** 6490
[28] Needs R J and Godfrey M J 1990 *Phys. Rev.* B **42** 10933
[29] Acioli P H and Ceperley D M 1996 *Phys. Rev.* B **54** 17199
[30] Cho J H, Ismail, Zhang Z and Plummer E W 1999 *Phys. Rev.* B **59** 1677
[31] Rydberg H, Lundqvist B I, Langreth D C and Dion M 2000 *Phys. Rev.* B **62** 6997
[32] Kiejna A and Pogosov V V 2000 *Phys. Rev.* B **62** 10445
[33] Nekovee M and Pitarke J M 2001 *Comput. Phys. Commun.* **137** 123
[34] Pitarke J M and Eguiluz A G 2001 *Phys. Rev.* B **63** 045116
[35] Halas S, Durakiewicz T and Joyce J J 2002 *Chem. Phys.* **278** 111
[36] Mugarza A and Ortega J E 2003 *J. Phys.: Condens. Matter* **15** S3281
[37] Fratesi G, Brivio G P and Molinari L G 2004 *Phys. Rev.* B **69** 245113
[38] Jiang Q, Lu H M and Zhao M 2004 *J. Phys.: Condens. Matter* **16** 521
[39] Razavy M, March N H and Paranjape B V 1996 *Phys. Rev.* B **54** 4492
[40] Jung J, García-González P, Dobson J F and Godby R W 2004 *Phys. Rev.* B **70** 205107
[41] Wigner E 1934 *Phys. Rev.* **46** 1002
[42] Wigner E 1938 *Trans. Faraday Soc.* **34** 678
[43] Care C M and March N H 1975 *Adv. Phys.* **24** 101
[44] Okazaki K and Teraoka Y 2001 *Appl. Surf. Sci.* **169/170** 48
[45] Foldy L L 1978 *Phys. Rev.* B **17** 4889
[46] Kholopov E V 2007 *J. Phys. A: Math. Theor.* to be published
[47] Sholl C A 1967 *Proc. Phys. Soc.* **92** 434
[48] Kholopov E V 2006 *Phys. Status Solidi* b **243** 1165
[49] Massidda V and Hernando J A 1980 *Physica* B **101** 159
[50] Madelung E 1918 *Phys. Z.* **19** 524
[51] Harris F E and Monkhorst H J 1970 *Phys. Rev.* B **2** 4400
[52] Brüesch P and Lietz M 1970 *J. Phys. Chem. Solids* **31** 1137